Neural Comput & Applic (2006)
DOI 10.1007/s00521-006-0049-7

ORIGINAL ARTICLE

Raimondo Schettini · Silvia Zuffi

A computational strategy exploiting genetic algorithms to recover color surface reflectance functions

Received: 17 February 2006 / Accepted: 3 March 2006

Abstract Information about the spectral reflectance of a color surface is useful in many applications. Assuming that reflectance functions can be adequately approximated by a linear combination of a small number of basis functions, we address here the recovery of a surface reflectance function, given the tristimulus values under one or more illuminants. Basis functions presenting different characteristics and cardinalities are investigated, and genetic algorithms are employed to optimize the estimation. Our analysis of a variety of standard datasets provides information about the ability of each set of basis functions we used to model generic reflectance spectra.

Keywords Genetic algorithms · Linear models · Reflectance function · Tristimulus values

1 Introduction

Information about the spectral reflectance of a color surface is useful in many applications. It can, for example, be helpful in simulating the change in appearance of a colored object under changing illuminants in CAD applications; or provide the input of computer programs for the matching color formulation of paints, inks, plastics, and textiles; or serve as input for many general computer graphics applications that require a wavelength-based approach to specify colors. Unfortunately, the surface reflectance is not often specified; most of the time, surface color information is given as RGB or XYZ tristimulus values.

In the physical world, spectra are functions defined over some continuous range of wavelengths. The representation most commonly employed is the uniform sampling of the visible spectrum, usually in the 400–700 nm range. Even when it provides for portability and, if a large number of samples are used, for accuracy as well, sampling is an impractical representation. In many applications, it may present the drawback of poor compactness when, to ensure accuracy, many samples are required. A number of researchers, e.g. [1–3], have investigated the modeling of reflectance spectra using dimensionality reduction techniques. These techniques exploit linear model representation, which expresses a reflectance spectrum through a weighted sum of a set of basis functions. These functions can be computed from a set of available spectra by applying principal component analysis (PCA) or independent component analysis, which offer accuracy and compactness, but may restrict the representation to a specific domain. Of considerable interest are representations where the set is composed of generic mathematical functions, providing for portability and avoiding the data acquisition and preprocessing required to compute data-dependent basis functions.

We address here the problem of estimating plausible reflectance spectra from tristimulus values for a variety of representations of reflectance functions through linear models. The main assumptions of our work are that the illuminant spectrum is known, that reflectance spectra are smooth functions of wavelength in the range of reflectance values between 0 and 100, and that no phenomena of fluorescence occur. Linear models represent reflectance functions with a good to high degree of accuracy, depending on the number of basis functions considered. There are many studies on the dimensionality of linear models based on PCA for real reflectance spectra approximation. In general, for natural surfaces, a dimension of six to nine bases is considered sufficient [1, 3, 4], while, for skin reflectance, three basis functions are enough [5]. Most of the methods available for the

R. Schettini
DISCo (Dipartimento di Informatica, Sistemistica e Comunicazione),
Università degli Studi di Milano-Bicocca,
Via Bicocca degli Arcimboldi, 8, 20126 Milan, Italy

S. Zuffi (✉)
Construction Technologies Institute, ITC-CNR,
Via Bassini 15, 20133 Milan, Italy
E-mail: zuffi@itc.cnr.it

estimation of reflectance from tristimulus values assume it is possible to represent the spectral reflectance functions with a three-dimensional linear model, e.g. [6–9], do not allow the simultaneous exploitation of tristimulus values referred to different illuminants, and employ a fixed pre-defined set of basis functions to model reflectance spectra. In this paper we investigate whether better reflectance estimates can be achieved relaxing these assumptions.

The approximation of reflectance functions may, in general, gain in accuracy from the use of high-dimensional linear models: the linear combination of the model's basis functions can better match the given reflectance spectrum. In estimating a surface reflectance function from tristimulus values, the linear model taken to represent the unknown reflectance function must not only provide the high level of flexibility required for spectral matching, but also encode some knowledge or constraints regarding the characteristics of the function to estimate. Colorimetric tristimulus values encode information about the surface physics of reflectance at each wavelength as a triplet of values, which includes observer and illuminant characteristics. As an infinite number of different reflectance functions can produce the same triplet, the problem of reflectance synthesis may have infinite solutions. In order to compensate partially for the insufficient information provided by colorimetric data, linear models with basis components computed on suitable datasets are used. Unfortunately, using three PCA basis functions to estimate a reflectance spectrum from tristimulus values may still not offer a good solution. While the reflectance spectrum obtained may be perfectly metameric with respect to the unknown spectrum under the given illuminant and with the given observer, it may exhibit poor colorimetric matching with a different illuminant or observer, indicating that the underlying spectral match required has not been obtained. Since the spectral matching cannot be addressed directly, a method that allows the synthesis of a surface reflectance spectrum by taking into account colorimetric information referred to different illumination or observation conditions can increase the similarity between the estimated and the unknown reflectance spectrum. We have applied genetic algorithms (GA) to formulate the problem of reflectance estimation for the simultaneous optimization of several constraints. We based our approach on GA as they are a general method to solve optimization problems, allowing the formulation of the recovery problem in a simple way, similar for all the different formulations investigated. GA have performances comparable with other techniques [10], and are appropriate for complex non-linear models where the location of the global minimum is a difficult task [11]. Genetic algorithms have been applied here to design a single computational framework to surface reflectance function recovery, where any kind of basis components in variable number can be adopted.

In Sect. 2 we provide a formal formulation of the problem addressed. Section 3 describes the basis functions considered here, while Sect. 4 is a brief overview of the GA proposed. The performance of the algorithm and of the basis functions is examined in Sect. 5, where standard datasets are used for benchmarking.

2 Problem formulation

A color stimulus is related to the CIE XYZ tristimulus values by the following equations:

$$\begin{aligned} X &= K\int_{\lambda} R(\lambda)I(\lambda)\bar{x}(\lambda)\ \mathrm{d}\lambda \\ Y &= K\int_{\lambda} R(\lambda)I(\lambda)\bar{y}(\lambda)\ \mathrm{d}\lambda \\ Z &= K\int_{\lambda} R(\lambda)I(\lambda)\bar{z}(\lambda)\ \mathrm{d}\lambda \end{aligned} \tag{1}$$

where $R(\lambda)$ is the reflectance spectrum, $I(\lambda)$ is the illuminant's spectral power distribution, $\bar{x}(\lambda)$, $\bar{y}(\lambda)$ and $\bar{z}(\lambda)$ are the color matching functions that define the CIE 1931 standard colorimetric observer. If the reflectance function is represented in the range of [0,1], and a luminance of 100 is attributed to the light source in the scene, then the normalization factor K is:

$$K = \frac{100}{\int_{\lambda} I(\lambda)\bar{y}(\lambda)\ \mathrm{d}\lambda}. \tag{2}$$

Equation 1 indicates that an infinite number of different reflectance functions may generate the same tristimulus values. The reflectance function may be expressed through a linear model as a weighted sum of a set of basis functions:

$$R(\lambda) = \sum_{j=1}^{\tilde{N}} w_j b_j(\lambda) \tag{3}$$

where $\tilde{N}$ is the number of bases in the linear model, $b_j(\lambda)$ is the base function of index j, and w_j is the corresponding weight. We have considered $\lambda_{\min} = 400$ nm, $\lambda_{\max} = 700$ nm and $\Delta\lambda = 10$ nm here. Approximating the three integrals in Eqs. 1 as summations over a limited range of wavelengths, and applying Eq. 3, the tristimulus values equations become

$$\begin{aligned} X &= K\sum_{\lambda_{\min}}^{\lambda_{\max}}\sum_{j=1}^{\tilde{N}} w_j b_j(\lambda)I(\lambda)\bar{x}(\lambda)\Delta\lambda \\ Y &= K\sum_{\lambda_{\min}}^{\lambda_{\max}}\sum_{j=1}^{\tilde{N}} w_j b_j(\lambda)I(\lambda)\bar{y}(\lambda)\Delta\lambda \\ Z &= K\sum_{\lambda_{\min}}^{\lambda_{\max}}\sum_{j=1}^{\tilde{N}} w_j b_j(\lambda)I(\lambda)\bar{z}(\lambda)\Delta\lambda. \end{aligned} \tag{4}$$

If we indicate with **B** the matrix having as columns the basis vectors, and with **w** the weights column vector, then, Eq. 3 can be written in matrix notation as:

$$\mathbf{R} = \mathbf{B}\mathbf{w}. \tag{5}$$

Denoting with **S** the column vector of tristimulus values $[X\ Y\ Z]^{\mathrm{T}}$, if $\bar{\mathbf{s}}$ is the matrix having as columns the observer sensitivities, and diag(**I**) is a matrix having the illuminant's spectral power distribution in the diagonal and zero elsewhere, then

$$\mathbf{S} = \mathrm{K}\ \bar{\mathbf{s}}^{\mathrm{T}}\ \mathrm{diag}(\mathbf{I})\mathbf{R}\Delta\lambda \tag{6}$$

and, substituting Eq. 5 in Eq. 6:

$$\mathbf{S} = \mathrm{K}\ \bar{\mathbf{s}}^{\mathrm{T}}\ \mathrm{diag}(\mathbf{I})\mathbf{B}\mathbf{w}\Delta\lambda. \tag{7}$$

We must now find the weights in Eq. 7, given the tristimulus values and assuming that no fluorescence occurs. Once the weights have been estimated, the reflectance spectrum can be computed using Eq. 5. The estimated reflectance function must be feasible, that is in the range of [0, 100], and minimize the color difference between the input color, specified by a given XYZ triplet together with the corresponding illuminant spectral power distribution, and the tristimulus values computed using Eq. 7. We considered different types of basis sets, all of which require the estimation of a variable number of parameters.

3 The basis sets considered

The different sets of basis functions experimented included those obtained by PCA performed on the datasets studied and on Vrhel's public domain database of natural color reflectances [13], Fourier basis functions, and Gaussian basis functions. Basis sets obtained by PCA are particularly interesting, as they have already been used to model reflectance functions in many applications. PCA is a data-driven analysis, and in most of the cases the basis components are derived by the considered dataset. But in many applications one cannot assume the knowledge of a suitable dataset including the color under investigation. It is therefore a frequently adopted solution that of considering generic dataset among the many of measured reflectance spectra available in literature or that of adopting generic functions as basis components. In literature, datasets commonly used are the Munsell Atlas and the Vrhel dataset, which have been considered in our investigation. Methods based on generic basis functions used Fourier and Gaussian functions. A major question in the problem formulation is the number of bases to consider. Studies on PCA have indicated that six components are sufficient for natural surfaces. Considering Fourier functions, in an early study by Wandell [17], where the surface reflectances of a set of 462 Munsell chips have been modeled with a three-dimensional linear system composed of Fourier basis functions, a rather good fit between measured spectra and linear model representations was observed. Regarding Gaussian functions, a number of three to five functions was used to model skin reflectance. It has to be underlined, however, that most of the studies on the dimensionality of linear models evaluate a degree of fit between the reflectance function and its representation in the wavelength domain. But the problem of representing a given spectrum is different from the problem of recovery a spectrum given the outputs of some photoreceptors or filters. According to Maloney, in fact, surface spectral reflectances fall within a linear model composed by five to seven parameters (basis reflectance vectors), but when the effect of human photoreceptors sensitivities is included, linear model with as few as three to four parameters provide excellent fit to the data sets [3]. Our approach here was to design linear models considering basis functions in accordance with previous studies, exploiting the possibility offered by GA to consider a variable number of basis components.

3.1 Principal components analysis

Principal component analysis allows the computation of basis functions for linear model representation. A PCA basis set corresponds to directions having maximum variance in the data space; the idea is to account for the direction in which the measured data has the most variance. The use of PCA implies the assumption that the distribution of the data has a Gaussian form.

Given **R**, a matrix where the columns are reflectance vectors, we consider **X**, a translation of R centered around mean value of the reflectances. If N is the number of wavelength samples, the PCA identifies a set of $\tilde{N}$ vectors $\mathbf{b}_j$ corresponding to the direction, in N-dimensional space, in which the reflectance vectors exhibit maximum variance. These vectors define an orthogonal basis of a sub-space of dimension $\tilde{N}$.

The basis set vectors are computed as the first $\tilde{N}$ eigenvectors, corresponding to the first $\tilde{N}$ largest eigenvalues, of $\frac{1}{P}\mathbf{X}\mathbf{X}^{\mathrm{T}}$, where P is the number of reflectance vectors.

The number of components needed to accurately represent a set of reflectance spectra depends on the characteristics of the data set. The reflectance spectra of most objects found in nature are smooth functions of wavelength; the same is true of spectra produced using photography, printing, or paints. These spectra can, therefore, be accurately represented by a limited number of basis functions [14]. Various studies have estimated that three to seven principal components will provide a satisfactory reconstruction of the reflectance spectra in most cases, while increasing the number does not guarantee a better performance [15].

We have set the number of basis functions at six, in accordance with Maloney [3], who has demonstrated

that a linear model with as few as six basis functions provides essentially perfect fits for almost all natural surface spectral reflectance functions.

Consequently the reflectance function here is represented by the following equation:

$$R(\lambda) = \sum_{j=1}^{6} A_j b_j(\lambda) \tag{8}$$

where $b_j(\lambda)$ is the basis function of index j, and A_j is the corresponding weight.

3.2 Fourier basis set

In the Fourier transform, a generic signal can be represented with a series of trigonometric functions. For a reflectance spectrum defined in the visible range of $L = \lambda_{\max} - \lambda_{\min}$, the Fourier expansion has the general form:

$$R(\lambda) = \frac{a_0}{2} + \sum_{n=1}^{\infty} \left\{ a_n \cos\left[\frac{2\pi\, n(\lambda - \lambda_{\min})}{L}\right] + b_n \sin\left[\frac{2\pi\, n(\lambda - \lambda_{\min})}{L}\right] \right\} \tag{9}$$

As reported in [16], a set of three frequency-limited functions of wavelength can be used as a basis set for modeling spectra. The use of the first three Fourier functions has been proposed by Wandell [17] and applied, among others, by Schettini [18]. Fourier coefficients have also been employed by Sun et al. [19] to represent the smooth part of generic reflectance functions in their composite spectral model.

We have focused here on surface reflectances that can be regarded as smooth functions of wavelength; consequently we consider only basis functions having the property of smoothness. On an experimental basis we selected only the constant term, functions having frequency parameter $n = 1$, and two more functions having a period twice the spectrum range. We refer to this set here below as the "Fixed Fourier" (FF) case. The reflectance function is therefore represented by the following equation:

$$R(\lambda) = B_0 + B_1 \cos\left[\frac{2\pi(\lambda - \lambda_{\min})}{L}\right] + B_2 \sin\left[\frac{2\pi(\lambda - \lambda_{\min})}{L}\right] + B_3 \cos\left[\frac{\pi(\lambda - \lambda_{\min})}{L}\right] + B_4 \sin\left[\frac{\pi(\lambda - \lambda_{\min})}{L}\right] \tag{10}$$

where $L = \lambda_{\max} - \lambda_{\min}$ and B_0, B_1, B_2, B_3, B_4 are the weights of the linear model.

In a second analysis, we treated the basis function frequency as a tunable parameter, and also added a phase term. We have called this model the "Variable Fourier" (VF). The reflectance function is represented with the following equation:

$$R(\lambda) = C_0 + C_1 \cos\left[\frac{2\pi C_2(\lambda - \lambda_{\min})}{L} + 2\pi C_3\right] + C_4 \sin\left[\frac{2\pi C_5(\lambda - \lambda_{\min})}{L} + 2\pi C_6\right] \tag{11}$$

In this case, the unknowns in the reflectance spectrum representation are the weights C_0, C_1, and C_4, the frequency terms C_2 and C_5, and the phase terms C_3 and C_6.

3.3 Gaussian basis set

Angelopoulou et al. [22] have used an approximation of reflectance spectra with Gaussian functions to model skin reflectances. A Gaussian basis set has also been used by Dupont [23]. We considered a basis set composed of 15 Gaussian functions obtained with the following equation:

$$g_j(\lambda) = \exp\left[-4\,\ln(2)\frac{(\lambda - \lambda_j)^2}{40}\right] \quad j = 1, \ldots, 15 \tag{12}$$

where λ_j ranges from 400 to 700 with a step of 20. The reflectance function is represented by the equation

$$R(\lambda) = \sum_{j=1}^{15} D_j g_j(\lambda) \tag{13}$$

where D_j are the 15 weights of the linear model to be estimated.

We refer to this basis as the "Fixed Gaussian" case (FG). We have also investigated a "Variable Gaussian"(VG) approach, in which the reflectance function is modeled using a constant term and three Gaussian functions:

$$R(\lambda) = E_0 + E_1 \exp\left[-\frac{(((\lambda - \lambda_{\min})/L) - E_2)^2}{E_3^2}\right] + E_4 \exp\left[-\frac{(((\lambda - \lambda_{\min})/L) - E_5)^2}{E_6^2}\right] + E_7 \exp\left[-\frac{(((\lambda - \lambda_{\min})/L) - E_8)^2}{E_9^2}\right] \tag{14}$$

where the unknowns are the weights E_0, E_1, E_4, and E_7, the mean terms E_2, E_5, and E_8, and the terms E_3, E_6, and E_9 correlated with the standard deviation.

4 The genetic algorithm

Genetic algorithms (GA) are a general method for solving optimization problems, inspired by the mechanisms of evolution in biological systems (see e.g. [20, 21] for an introduction to GA and their applications). In the basic GA, every candidate solution is

represented by a sequence of binary, integer, real, or even more complex values, called an individual. A number of individuals are randomly generated as an initial population. The GA then iterates a procedure that produces a new population from the current one, until a given "STOP" criterion is satisfied. At each iteration, the value of a suitable "fitness" function is computed for every individual in the current population; the goal of the GA is to generate an individual with the best value of fitness. Given the problem described in Sect. 2, and assuming that only a triplet of tristimulus values is available, fitness is the squared sum of the perceptual differences between the CIELab values computed on the input color and those computed on the estimated reflectance spectrum, plus a term of range violation, with no perceptual meaning, to account for the bounds the solution must respect in order to match physical reflectance properties:

$$\text{fitness} = \left[(L^* - L^*_{\text{input,Ill}})^2 + (a^* - a^*_{\text{input,Ill}})^2 + (b^* - b^*_{\text{input,Ill}})^2 \right]_{\text{Ill}} + \delta_1(R(\lambda)) + \delta_2(R(\lambda)) \tag{15}$$

where $\delta_1(R(\lambda)) = D_1\left[\max_\lambda(R(\lambda)) - 100\right]$ iff $\max_\lambda(R(\lambda)) > 100$, else $\delta_1(R(\lambda)) = 0$ and $\delta_2(R(\lambda)) = -D_2\min_\lambda(R(\lambda))$ iff $\min_\lambda(R(\lambda)) < 0$, else $\delta_2(R(\lambda)) = 0$. In the equation, L^* is the lightness expressed in CIELab color space, subscript *input* indicates the input color coordinates, while subscript Ill indicates the illuminant considered to compute CIELab coordinates from reflectance.

Parameters D_1 and D_2 must be positive, and define the weight in the optimization function of the range violation error with respect to the colorimetric perceptual error. In our experiment we set $D_1 = D_2 = 1$. Therefore, range violation contributes to fitness to the same extent as the visual mismatch. These two quantities are inhomogeneous: range violation cannot be treated as a visual mismatch, because the filtering effect of observer sensitivities may preserve as acceptable a reflectance spectrum presenting out-of-range values in correspondence of a wavelength of poor observer sensitivity. No term of smoothness has been considered in the fitness function: the smoothness of the reflectance spectrum is not an issue, due to the characteristics of the linear model basis employed

GA, which can span the whole solution domain without halting at a local minimum, are considered more effective in estimating parameters than the less robust gradient descendent methods with random initialization. In our implementation, however, the robustness of the GA is reduced by the fact that the fitness function is not directly related to spectral matching. As said, many different spectra can generate the same XYZ triplet, and the GA does not have zenough information to select the best metameric reflectance function, that is the $R(\lambda)$ that not only has the smallest CIELAB error with respect to the input XYZ values, but also the smallest spectral error with respect to the actual $R(\lambda)$. None of the methods available for spectral estimation can escape this limitation. But if we assume that the tristimulus values referred to different illuminants are also known, a more effective fitness function can be designed:

$$\text{fitness} = \sum_{k=1}^{K} \left[(L^* - L^*_{\text{input,Ill}_k})^2 + (a^* - a^*_{\text{input,Ill}_k})^2 + (b^* - b^*_{\text{input,Ill}_k})^2 \right]_{\text{Ill}_k} + \delta_1(R(\lambda)) + \delta_2(R(\lambda)) \tag{16}$$

where K is the number of illuminants considered, and the other symbols are those used in Eq. 15.

To implement the GA, in our application we have used the public domain C++ library Galib [12], the GADeme class library, and fitness minimization in particular.

5 Experiments and results

Different data sets of reflectance functions have been used for benchmarking: the Macbeth ColorChecker Chart (a set of 24 paper patches used to calibrate imaging systems) and the whole Munsell Atlas [24]. These datasets have been used as benchmarks in several similar studies. Most programs for color recipe formulation require reflectance functions as input. Consequently, we have also tested the capability of our method in recovering the reflectance functions of a set of 120 Dupont paint chips [25] and of a set of 1,000 silk color samples spanning the range of feasible colors on that textile substrate, provided by a textile industry from its own collection. The silk dataset reflectance data can be also found in [26].

The following experiments were performed. For each dataset, given $R(\lambda)$ we computed the tristimulus values for three illuminants: D65 (a daylight spectral power distribution), A (a tungsten light), and F2 (a cool white fluorescence spectral power distribution). Then, for each type of basis set, we estimated the weights of Eq. 7 by means of a GA using the fitness function described in [16]. We conducted three experiments for each basis set and for each dataset: one considering only the D65 illuminant, a second considering the D65 and the A illuminants, and a third considering all three illuminants (D65, A and F2).

Genetic algorithms are randomly initialized; therefore, for each color, we made three runs of the method using different initializations, and selected the best solution in terms of the fitness value. In the GA, alleles are real numbers, and ranges must be defined for their

value. As described in the following paragraphs, these ranges have been arbitrarily selected, considering the characteristics of the basis set involved. However, if the GA gave as the best solution an individual with at least one allele at its domain border, a new run with the same initialization, but a larger domain, was performed. The GA employed had 20 parallel populations of 10 individuals; the stopping criteria was convergence; and mutation and crossover probabilities were set at 0.03 and 0.8, respectively, for all basis sets, except for the PCA and FG basis set, where the probabilities were 0.02 and 0.99. The results for the different basis sets are described in Sect. 3.

The PCA approach is in general applied when an appropriate dataset is available. As this is not always the case, we studied basis sets obtained by PCA performed on the studied datasets, and a basis set obtained from Vrhel's public domain database of natural color reflectances as well. We applied the latter to all the datasets used in our experiments in order to identify a standard set of PCA basis functions for the linear model representation of a generic reflectance spectrum.

5.1 PCA basis set

We computed four basis sets by applying PCA to the datasets used for benchmarking. We then estimated the reflectance spectra for each dataset, using the corresponding basis set.

In the GA, each individual was an array of 6 real numbers representing the weights of the six-dimension linear model; the bounds for each weight were assigned by computing the minimum and the maximum value assumed by the weight in the PCA representation of the dataset considered. We included, in the initial population, an individual that represents a perfect metameric solution, setting the first three weights at those computed by inverting the linear model in [5] with $\tilde{N} = 3$ number of basis, and the remaining three weights at zero. This signifies the presence of an individual of optimal fitness, if the corresponding spectrum is in the domain of [0, 100]. This strategy ensures that, since the first three basis functions are the most representative for the dataset considered, a metameric solution that is probably also a good spectral match with respect to the original reflectance will be found. If more than one illuminant is used, one individual in the initial population represents a perfect metameric solution with respect to the D65 illuminant. This solution is not necessarily an optimum, even if the corresponding spectrum has feasible values, since the metamerism does not in general hold for the second or third illuminant. Table 1 reports the statistics of results obtained using the PCA basis set of each dataset considered.

In Table 1, the results are reported as average error, maximum error and standard deviation of the distance in CIELAB space between the coordinates of the measured and the estimated spectra under the illuminants D65, A, and F2. The spectral mismatch is reported as the mean absolute error between reflectance spectra. Fitness values and out of range results are also reported. For each dataset, the first row reports the results for the estimation, assuming the tristimulus values for the D65 illuminant are available. In this case, the colorimetric error ΔE D65 is low, while colorimetric errors for the A and F2 illuminants are larger, and indicate that the estimated spectra are metameric with respect to the original ones. The use of two or three illuminants, as reported in the second and third row of each dataset, reduces the difference between colorimetric errors. As a consequence, the spectral error is also reduced.

5.2 PCA on the Vrhel database

The PCA method described above has been applied here, using the Vrhel database of natural surface reflectance as the training set for calculation of the basis components. Table 2 shows the statistics of the results.

Table 1 Statistics of results obtained using the PCA basis set of each of the dataset considered

PCA	ΔE D65			ΔE A			ΔE F2			MAE			Fitness			Out of range		
	Avg	M	SD	Avg	M	SD	Avg	M	SD	Avg	M	SD	Avg	M	SD	Avg	M	SD
Macbeth, D65	0.00	0.09	0.02	2.72	8.24	2.01	2.26	6.20	1.52	3.19	5.82	1.58	0.00	0.01	0.00	0.00	0.00	0.00
D65, A	0.19	0.60	0.14	0.20	0.51	0.14	0.75	1.79	0.54	2.15	5.11	1.10	0.11	0.54	0.15	0.00	0.00	0.00
D65, A, F2	0.18	0.66	0.14	0.26	0.94	0.20	0.32	1.02	0.27	1.66	5.50	1.03	0.33	2.04	0.49	0.00	0.00	0.00
Munsell, D65	0.00	0.08	0.01	1.67	9.73	1.50	1.32	8.69	1.18	1.81	8.57	1.30	0.00	0.01	0.00	0.00	0.00	0.00
D65, A	0.13	0.87	0.11	0.14	1.06	0.12	0.90	7.54	0.84	1.82	7.58	1.22	0.07	1.38	0.12	0.00	0.20	0.01
D65, A, F2	0.18	2.21	0.17	0.29	1.90	0.24	0.27	2.14	0.23	1.25	4.64	0.70	0.33	9.96	0.66	0.00	0.36	0.01
Dupont, D65	0.06	0.72	0.13	3.85	22.9	4.77	3.16	16.8	3.43	2.81	7.38	1.43	0.26	2.47	0.63	0.24	2.40	0.61
D65, A	0.35	1.55	0.36	0.40	2.62	0.48	2.28	17.9	2.98	1.98	6.10	1.13	0.91	9.12	1.7	0.27	3.09	0.67
D65, A,F2	0.47	2.68	0.58	0.77	7.55	1.07	0.79	6.35	1.09	1.48	5.69	0.79	4.21	100	11.7	0.14	2.77	0.43
Silk, D65	0.01	0.38	0.04	1.92	8.34	1.52	1.85	8.70	1.27	2.01	8.80	1.54	0.00	0.28	0.01	0.00	0.22	0.01
D65, A	0.23	1.13	0.18	0.24	1.54	0.19	1.28	7.72	1.17	1.66	7.96	1.21	0.18	3.24	0.32	0.01	2.18	0.10
D65, A,F2	0.28	1.29	0.21	0.46	3.17	0.37	0.47	2.49	0.36	1.55	7.77	1.14	0.83	16.8	1.31	0.01	1.43	0.07

MAE mean absolute error, *Avg* mean value, *M* maximum value, *SD* standard deviation

Table 2 Statistics of results obtained using the PCA basis computed on the Vrhel database of reflectances

PCA Vrhel	ΔE D65			ΔE A			ΔE F2			MAE			Fitness			Out of range		
	Avg	M	SD	Avg	M	SD	Avg	M	SD	Avg	M	SD	Avg	M	SD	Avg	M	SD
Macbeth, D65	0.01	0.07	0.02	2.64	9.63	2.23	2.23	8.70	1.93	3.35	7.34	1.72	0.00	0.01	0.00	0.00	0.00	0.00
D65, A	0.23	0.72	0.21	0.19	0.70	0.16	1.34	3.88	0.95	2.40	5.63	1.29	0.15	0.88	0.23	0.00	0.00	0.00
D65, A, F2	0.25	1.14	0.23	0.50	1.41	0.33	0.69	1.94	0.46	2.13	4.96	0.97	1.15	5.89	1.49	0.00	0.00	0.00
Munsell, D65	0.01	0.81	0.03	2.57	14.19	1.80	1.83	10.35	1.34	3.48	12.23	2.24	0.00	1.23	0.04	0.00	1.16	0.04
D65, A	0.18	1.47	0.18	0.16	1.25	0.15	1.17	10.53	1.00	2.44	8.61	1.48	0.11	3.66	0.26	0.00	2.14	0.06
D65, A, F2	0.21	1.65	0.15	0.38	2.08	0.30	0.57	2.69	0.42	1.39	3.62	0.77	0.81	11.3	1.21	0.02	3.96	0.21
Dupont, D65	0.07	0.65	0.13	2.72	10.67	2.10	2.55	8.95	2.14	3.25	11.22	2.17	0.44	10.6	1.45	0.42	10.5	1.43
D65, A	0.36	1.86	0.41	0.49	2.74	0.62	2.08	8.10	2.0	2.69	9.63	1.71	1.43	24.7	3.27	0.52	16.2	1.85
D65, A, F2	0.562	3.14	0.69	0.81	3.53	0.81	1.21	4.54	1.20	2.54	9.63	1.65	5.54	39.3	8.92	0.55	14.9	1.81
Silk, D65	0.02	0.54	0.06	2.61	10.88	2.10	2.31	12.75	1.87	4.16	11.69	2.26	0.06	12.9	0.58	0.05	12.8	0.57
D65, A	0.25	1.50	0.22	0.24	2.60	0.24	1.54	10.17	1.35	3.24	10.06	1.64	0.32	25.3	1.43	0.10	20.9	1.00
D65, A, F2	0.27	2.45	0.22	0.55	3.43	0.44	0.75	3.67	0.56	2.86	10.34	1.30	1.62	38.5	3.02	0.13	18.1	0.96

MAE mean absolute error, *Avg* mean value, *M* maximum value, *SD* standard deviation

In this case as well, the spectral match benefits from the use of more than one illuminant: for each dataset, the mean absolute error has the lowest values when all three illuminants are used. The errors in estimation of the reflectance functions are in general bigger than those found in Table 1.

5.3 Fourier basis set

In the fixed Fourier (FF) case, each individual of the GA is an array of five real numbers, with bounds of [0, 100] for the first element, corresponding to an offset term, and of [–30, 30] for the remaining four weights of the trigonometric functions. When Fourier functions with variable parameters are used (VF), the individuals are arrays of 7 real numbers, with ranges of [0, 100] for the offset term, of [–30, 30] for the amplitudes, of [0.1, 1.2] for the frequency terms, and of [0, 1] for the phase terms. Table 3 reports the statistics of the results obtained using the FF basis set, while Table 4 registers those obtained with the VF basis set.

These results indicate that the FF and the VF basis behave in a similar manner, the performance of the variable set being only slightly worse, as can be seen in Fig. 1. The sum of the average mean absolute error for each dataset is reported for the three experiments performed with the FF basis (left) and the VF basis (right). The diagram shows that, in general, increasing the number of illuminants decreases the spectral error, but the difference is negligible in the case of VF when passing from two to three illuminants.

Figure 2 presents an example of reflectance estimation using the VF basis set. The measured and the estimated reflectance function of the fourth color sample in the Dupont dataset are given, from when is clearly seen that the match between measured and estimated functions is best when all three illuminants are used.

5.4 Gaussian basis set

In the FG case, each individual is an array of 15 real numbers, with bounds of [0, 1]. When Gaussian functions with variable parameters (VG) are used, individuals are arrays of 10 real numbers, with ranges of [0, 100] for the offset term, of [−30, 30] for the

Table 3 Statistics of results obtained using the Fixed Fourier basis set

Fixed Fourier	ΔE D65			ΔE A			ΔE F2			MAE			Fitness			Out of range		
	Avg	M	SD	Avg	M	SD	Avg	M	SD	Avg	M	SD	Avg	M	SD	Avg	M	SD
Macbeth, D65	0.02	0.21	0.05	3.45	10.2	3.03	2.83	8.57	2.60	5.51	16.5	4.07	0.01	0.26	0.05	0.01	0.23	0.05
D65, A	0.47	2.28	0.52	0.52	3.53	0.72	1.77	4.96	1.51	3.11	7.85	1.98	1.28	18.4	3.73	0.03	0.73	0.15
D65, A, F2	0.69	3.25	0.73	0.82	2.96	0.83	1.01	2.95	0.90	2.78	7.98	1.81	4.20	28.6	6.78	0.10	1.14	0.29
Munsell, D65	0.01	0.61	0.03	2.84	12.9	1.95	1.99	9.08	1.40	4.32	14.0	2.29	0.02	5.13	0.23	0.01	5.05	0.22
D65, A	0.35	2.79	0.33	0.36	4.50	0.40	1.28	9.14	1.15	2.66	10.7	1.79	0.56	28.1	1.64	0.05	10.5	0.47
D65, A, F2	0.48	4.25	0.52	0.61	4.29	0.53	0.76	3.80	0.71	2.40	10.6	1.64	2.30	52.2	4.11	0.08	12.2	0.66
Dupont, D65	0.13	1.54	0.23	4.57	22.6	4.77	3.43	14.4	2.95	5.05	12.1	2.80	1.30	11.3	2.45	1.24	11.2	2.36
D65, A	1.13	6.16	1.39	1.32	7.48	1.77	2.81	8.13	2.31	3.88	11.5	2.62	9.14	94.3	19.1	1.11	12.6	2.43
D65, A, F2	1.28	7.41	1.65	1.73	7.33	1.86	1.89	6.68	1.73	3.60	11.6	2.29	18.5	152	31.0	1.23	12.0	2.52
Silk, D65	0.02	0.62	0.06	3.54	12.1	2.43	2.63	11.8	1.86	5.09	16.6	3.05	0.15	8.17	0.79	0.14	8.08	0.78
D65, A	0.52	4.50	0.54	0.58	5.04	0.71	1.65	7.95	1.51	3.30	10.0	1.73	1.59	47.4	4.42	0.20	12.7	0.99
D65, A, F2	0.73	4.97	0.77	0.79	5.28	0.77	0.96	5.51	0.93	3.17	9.75	1.63	4.42	84.3	9.05	0.29	15.1	1.37

MAE mean absolute error, *Avg* mean value, *M* maximum value, *SD* standard deviation

Table 4 Statistics of results obtained using the variable Fourier basis set

Variable Fourier	ΔE D65			ΔE A			ΔE F2			MAE			Fitness			Out of range		
	Avg	M	SD	Avg	M	SD	Avg	M	SD	Avg	M	SD	Avg	M	SD	Avg	M	SD
Macbeth, D65	0.02	0.18	0.04	2.51	9.51	2.91	2.18	8.92	2.50	3.75	12.0	3.12	0.04	0.86	0.17	0.03	0.83	0.17
D65, A	0.66	3.39	0.81	0.77	5.33	1.21	1.84	6.51	1.77	3.06	7.37	2.18	3.08	40.5	8.46	0.02	0.55	0.11
D65, A, F2	0.85	5.04	1.29	1.04	5.04	1.22	1.17	3.95	1.12	3.02	7.80	2.14	7.47	67.2	15.3	0.10	1.45	0.34
Munsell, D65	0.01	0.26	0.02	1.92	10.4	1.85	1.51	10.6	1.43	3.03	15.4	2.36	0.01	2.95	0.11	0.01	2.93	0.11
D65, A	0.38	3.52	0.45	0.40	5.35	0.59	1.22	6.34	1.16	2.48	10.3	2.01	0.88	42.4	3.16	0.02	4.27	0.23
D65, A, F2	0.52	5.81	0.72	0.60	5.66	0.65	0.77	4.71	0.77	2.30	12.0	1.89	2.77	89.7	6.70	0.03	5.05	0.27
Dupont, D65	0.11	1.29	0.21	5.21	29.3	6.53	3.30	16.1	3.62	4.99	14.9	3.56	1.35	10.6	2.60	1.29	10.5	2.51
D65, A	1.54	9.83	2.37	1.66	10.8	2.63	3.00	11.0	2.85	4.22	13.0	2.92	18.6	193	43.5	1.07	8.01	1.91
D65, A, F2	1.74	10.4	2.60	2.13	11.5	2.83	2.07	9.09	2.23	3.93	12.4	2.74	32.5	323	66.8	1.14	7.95	2.09
Silk, D65	0.02	0.44	0.05	3.18	19.2	2.21	2.30	13.3	1.87	5.17	15.7	2.66	0.17	8.84	0.88	0.16	8.82	0.87
D65, A	0.73	6.56	0.79	0.83	7.92	1.06	1.86	10.7	1.50	3.81	11.7	1.93	3.17	98.8	10.3	0.21	10.6	0.95
D65, A, F2	0.83	8.09	1.08	1.03	6.91	1.04	1.19	6.63	1.08	3.71	10.6	1.90	6.84	161	17.1	0.27	14.3	1.22

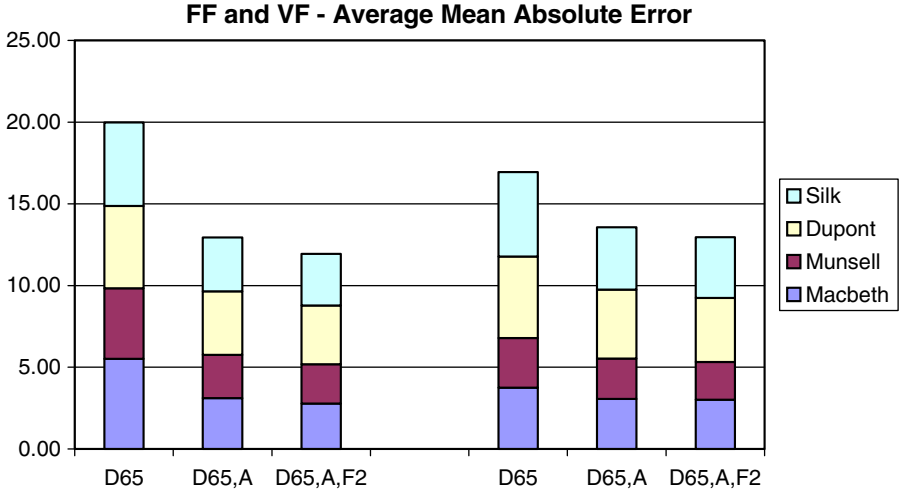

Fig. 1 Sum of the average mean absolute error for each dataset (*y*-axis), for the three experiment performed, and for the FF basis (*left*) and VF basis (*right*) (*x*-axis)

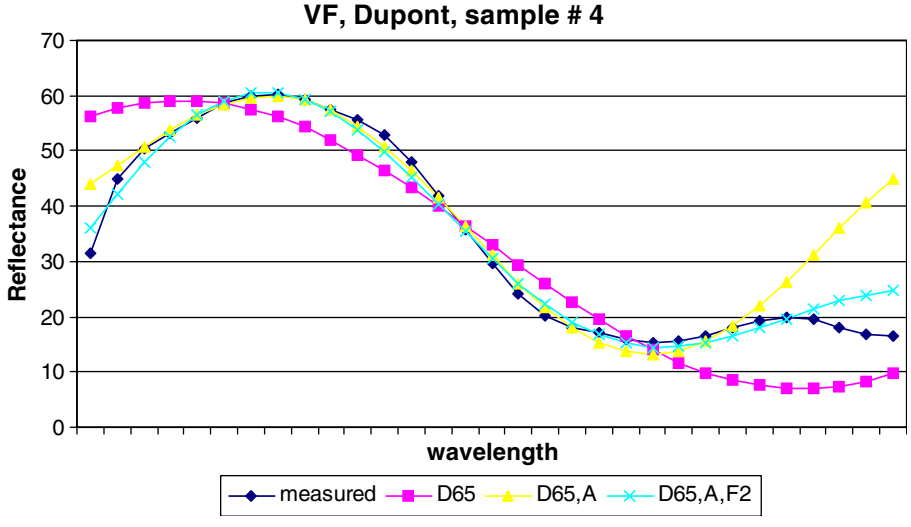

Fig. 2 Example of reflectance estimation for the fourth sample of the Dupont dataset, using the variable Fourier basis set and different sets of illuminants

amplitudes, of [−0.5, 1.5] for the mean terms, and of [0.1, 0.8] for the terms correlated with the standard deviation. Table 5 reports the statistics of results obtained using the fitness in Eqs. 4 and 5, and the FG basis set. Tables 6 shows the statistics of the results obtained employing the VG basis set.

Table 5 Statistics of results obtained using the Fixed Gaussian basis set

Fixed Gaussian	ΔE D65			ΔE A			ΔE F2			MAE			Fitness			Out of range		
	Avg	M	SD	Avg	M	SD	Avg	M	SD	Avg	M	SD	Avg	M	SD	Avg	M	SD
Macbeth, D65	0.13	0.45	0.11	3.87	9.13	2.60	3.19	5.67	1.51	5.68	10.2	2.94	0.03	0.20	0.05	0.00	0.00	0.00
D65, A	0.45	1.03	0.23	0.43	1.06	0.22	1.92	4.25	0.96	3.66	9.04	1.95	0.49	2.18	0.50	0.00	0.00	0.00
D65, A, F2	0.45	1.11	0.24	0.53	2.25	0.44	0.69	1.76	0.42	3.09	7.45	1.72	1.37	8.88	1.81	0.00	0.00	0.00
Munsell, D65	0.12	0.81	0.10	4.44	14.3	2.90	3.47	10.0	1.82	6.43	18.3	3.57	0.02	0.65	0.05	0.00	0.00	0.00
D65, A	0.38	1.62	0.21	0.36	1.33	0.19	1.67	6.21	0.98	3.35	11.7	1.98	0.35	3.91	0.38	0.00	0.00	0.00
D65, A, F2	0.41	1.67	0.26	0.46	1.87	0.27	0.58	2.17	0.32	2.59	8.36	1.54	0.96	8.29	0.97	0.00	0.00	0.00
Dupont, D65	0.19	2.56	0.33	3.16	11.3	2.15	2.36	9.58	1.48	5.28	16.2	3.45	0.14	6.54	0.70	0.00	0.00	0.00
D65, A	0.49	2.68	0.40	0.47	2.05	0.40	1.51	3.79	0.80	3.41	11.9	2.26	0.78	11.4	1.54	0.00	0.00	0.00
D65, A, F2	0.53	2.57	0.43	0.64	2.28	0.46	0.73	2.60	0.50	2.96	7.31	1.89	1.86	10.6	2.30	0.00	0.00	0.00
Silk, D65	0.16	1.43	0.16	3.71	14.3	2.52	3.08	9.88	1.66	5.17	15.8	2.84	0.05	2.06	0.14	0.00	0.00	0.00
D65, A	0.43	2.40	0.27	0.42	2.46	0.26	1.68	6.58	0.99	3.79	10.8	1.99	0.50	11.8	0.71	0.00	0.00	0.00
D65, A, F2	0.51	3.57	0.35	0.55	2.37	0.32	0.66	2.88	0.36	3.42	10.6	1.76	1.35	20.6	1.54	0.00	0.00	0.00

MAE mean absolute error, *Avg* mean value, *M* maximum value, *SD* standard deviation

Table 6 Statistics of results obtained using the variable Gaussian basis set

Variable Gaussian	ΔE D65			ΔE A			ΔE F2			MAE			Fitness			Out of range		
	Avg	M	SD	Avg	M	SD	Avg	M	SD	Avg	M	SD	Avg	M	SD	Avg	M	SD
Macbeth, D65	0.00	0.01	0.00	1.93	7.50	2.03	1.71	7.38	2.04	2.95	9.01	2.40	0.00	0.00	0.00	0.00	0.00	0.00
D65, A	0.24	0.75	0.23	0.23	0.62	0.21	1.43	4.09	1.37	2.67	9.84	2.42	0.31	0.83	0.21	0.20	0.94	0.27
D65, A, F2	0.43	1.49	0.43	0.45	1.76	0.52	0.56	1.51	0.47	2.35	6.26	1.71	0.39	0.88	0.25	1.36	5.90	1.77
Munsell, D65	0.00	0.25	0.01	2.26	11.2	1.89	1.77	10.4	1.52	3.10	15.2	2.05	0.00	0.10	0.00	0.00	0.04	0.00
D65, A	0.18	1.02	0.16	0.18	1.44	0.18	0.94	10.9	0.87	2.08	10.6	1.54	0.12	3.34	0.29	0.00	1.36	0.05
D65, A, F2	0.26	2.79	0.27	0.30	2.34	0.28	0.38	2.88	0.32	1.85	9.61	1.33	0.56	15.51	1.17	0.00	0.89	0.03
Dupont, D65	0.04	1.07	0.12	3.20	18.5	3.17	2.16	9.83	1.96	3.87	11.7	2.36	0.26	6.16	0.91	0.25	6.08	0.88
D65, A	0.32	2.70	0.43	0.37	3.95	0.61	1.25	4.24	1.05	2.98	12.4	2.26	0.88	22.77	3.14	0.09	3.34	0.38
D65, A, F2	0.41	3.92	0.50	0.50	5.03	0.69	0.53	2.45	0.50	3.02	10.6	2.35	1.78	48.90	5.26	0.12	3.62	0.48
Silk, D65	0.01	0.73	0.05	3.08	11.5	2.15	2.43	12.4	1.90	5.14	17.5	2.84	0.08	7.39	0.55	0.08	7.33	0.53
D65, A	0.28	2.50	0.28	0.30	4.22	0.38	1.52	12.0	1.44	3.68	12.5	2.23	0.43	25.61	1.72	0.04	9.36	0.44
D65, A, F2	0.42	4.72	0.48	0.47	5.55	0.52	0.62	5.00	0.63	3.16	10.4	1.94	1.69	67.15	4.72	0.02	2.65	0.18

MAE mean absolute error, *Avg* mean value, *M* maximum value, *SD* standard deviation

The variable basis set performs better here than the fixed set of Gaussian functions, as can be observed by comparing Tables 3 and 4, and looking at Fig. 3. Figure 4 presents an example of reflectance estimation using the VG basis set is given. The measured and estimated reflectance function of the fourth color sample in the Dupont dataset are reported. It can be easily seen that the match between the measured and the estimated functions is best here as well when all three illuminants are used.

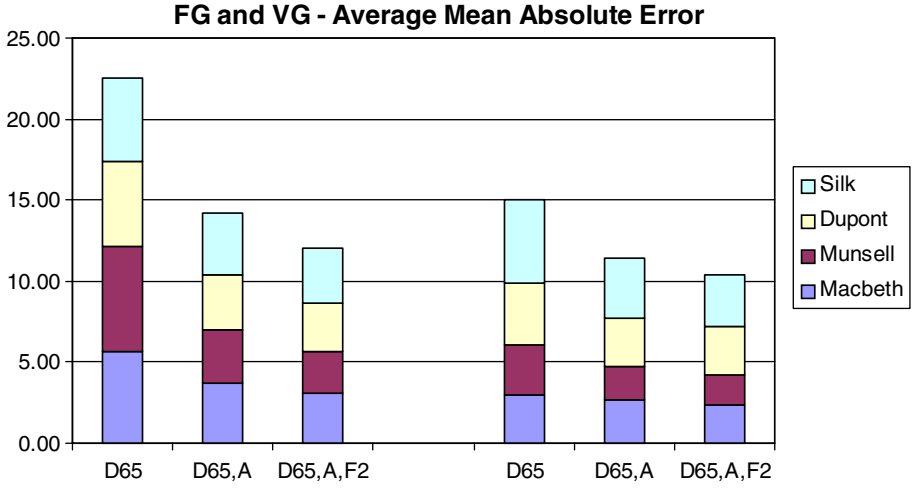

Fig. 3 Sum of the average mean absolute error for each dataset (*y*-axis), for the three experiments performed, using the FG basis (*left*) and the VG basis (*right*) (*x*-axis)

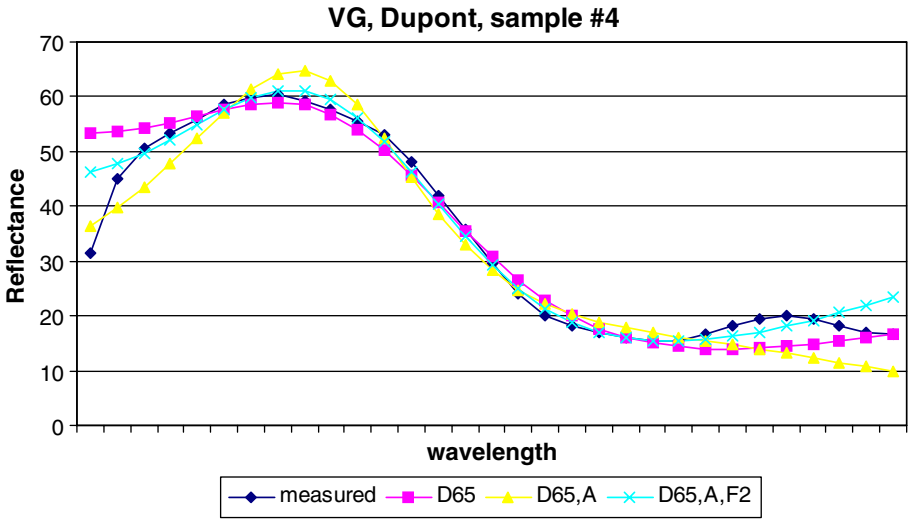

Fig. 4 Example of reflectance estimation for the fourth sample of the Dupont dataset, using the variable Gaussian basis set and different sets of illuminants

6 Discussion

Examining and comparing the results described in the previous section and the average errors registered, several observations can be made:

1. When only one illuminant (D65) is considered, the color error, in terms of Euclidean distance between the real and the estimated color in the color space of CIELAB coordinates under the same illuminant, is at its minimum. The error is considerably larger under different illuminants (A and F2). Adding a second illuminant (A), the color error for the first illuminant (D65) increases, while decreasing for the second and the third (A and F2). It further decreases with the addition of the third illuminant (F2) but the improvement is less marked than that made by adding the second illuminant (A) in the fitness function. This holds for all the datasets and basis sets considered.
2. In general, using a fitness function that simultaneously minimizes the color error under different illuminants improves the spectral match between the original spectra and those estimated.
3. Taking the spectral match as a measure of basis performance, when a training set is available, the basis functions computed using PCA outperform all the other sets.
4. When a training set is not available, the use of the basis set computed by PCA on the Vrhel database provides a better performance than either the Fourier or the Gaussian basis sets. This can be seen in Fig. 5, where the average mean absolute error for each basis set is plotted, and where each vertical line refers to a dataset, in the order: Macbeth, Munsell, Dupont, Silk.

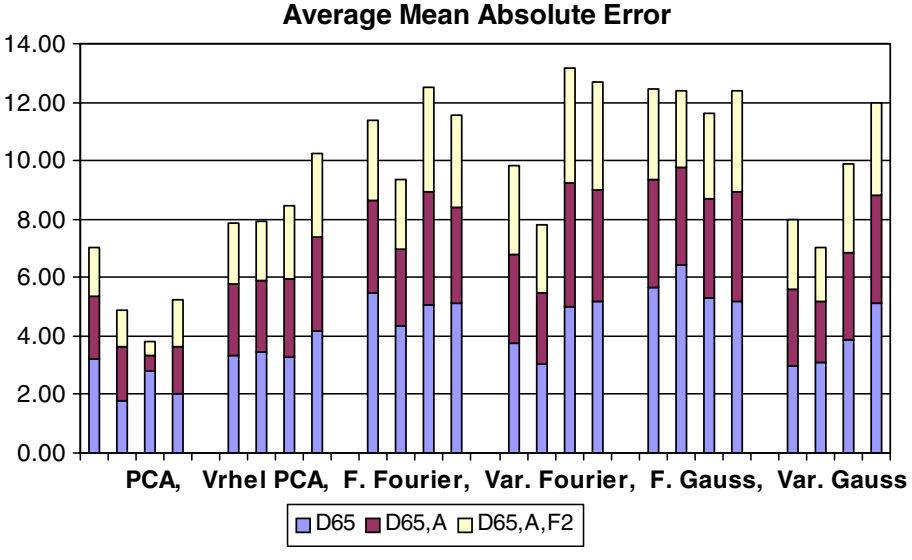

Fig. 5 Plot of the average mean absolute error for each basis set. For each basis set, each vertical line refers to one of the four datasets used for benchmarking, in the order: Macbeth, Munsell, Dupont, and Silk

These results demonstrate that the best performance is obtained when the functions computed from PCA of the input dataset are used as the basis set. Since, unfortunately, this information is not always available, a second choice for representing the reflectance functions could be the basis set computed on the Vrhel database, or on the VG basis set.

7 Conclusion

Assuming that reflectance functions can be adequately approximated by a linear combination of a small number of basis functions and exploiting GA, we address here the problem of synthesizing a spectral reflectance function, given the standard CIE 1931 tristimulus values. Within the CIE 1931 tristimulus equations, we describe reflectance functions with a large number of parameters, and use GA to estimate reflectance functions taking into account additional constraints about the actual feasibility of the estimated solutions.

We have investigated different types of basis functions for the linear model, and different datasets for benchmarking. No single set of basis functions can perfectly model all reflectance functions. Our results confirm that PCA basis sets provide the most effective approach to the problem. These results also indicate that when a suitable set of reflectance data for the calculus of PCA basis functions is lacking, a Gaussian basis set may be satisfactorily employed instead. Future research will be devoted to the analysis of general basis sets for surface reflectance modeling and to the application of our computational strategy to the recovery of surface reflectance functions from low-dimensional device responses.

References

1. Cohen J (1964) Dependency of the spectral reflectance curves of the Munsell color chips. Psycon Sci 1:369–370
2. Marimont DH, Wandell BA (1992) Linear models of surface and illuminant spectra. J Opt Soc Am 9(11):1905–1913
3. Maloney LT (1986) Evaluation of linear models of surface spectral reflectance with a small number of parameters. J Opt Soc Am A 3:1673–1683
4. Jaaskelainen T, Parkkinen J, Toyooka S (1990) A vector-subspace model for color representation. J Opt Soc Am A 7:725–730
5. Sun Q, Fairchild MD (2001) Statistical characterization of spectral reflectances in spectral imaging of human portraiture. In: The Is&T/Sid 9th color imaging conference, November
6. Sun Y, Fracchia FD, Calvert TW, Drew MS (1999) Deriving spectra from colors and rendering light interface. IEEE Comput Graph Appl
7. Cheng F, Hsu W, Chen T (1998) Recovering colors in an image with chromatic illuminant. IEEE Trans Image Processing 7(11):1524–1533
8. Schettini R (1994) Deriving spectral reflectance functions of computer-simulated object colors. Comput Graph Forum 13(4):211–217
9. Ho J, Funt BV, Drew MS (1990) Separating a color signal into illumination and surface reflectance components: theory and applications. IEEE Trans Pattern Anal Mach Intell 12(10):966–973
10. Mitchell M, Holland JH, Forrest S (1994) When will a genetic algorithm outperform hill climbing. In: Cowan JD, Tesaino G, Alspector J (eds) Advances in neural information processing systems, vol 6. Morgan Kaufmann, San Mateo, pp 51–58
11. Mardle S, Pascoe S (1999) An overview of genetic algorithms for the solution of optimisation problems. Comp In Higher Education Economics Review, 13/1
12. Galib: A C++ Library of genetic algorithm components, http://www.lancet.mit.edu/ga/
13. Vrhel MJ, Gershon R, Iwan LS (1994) Measurement and analysis of object reflectance spectra. Color Res Appl 19(1):4–9
14. Sharma G, Trussel HJ (1997) Digital color imaging. IEEE Trans Image Processing 6(7):901–932
15. Connah D, Westland S, Thomson MGA (2001) Recovering spectral information using digital camera systems. J Color Technol 117:309–312
16. Drew MS, Funt BV (1992) Natural metamers. Comput Vis Graph Image Process Image Understand 56(2):139–151
17. Wandell BA (1987) The synthesis and analysis of color images. IEEE Trans Pattern Anal Mach Intell 9:2–13
18. Schettini R, Barolo B (1996) Estimating reflectance functions from tristimulus values. Appl Signal Process 3:104–115
19. Sun Y, Fracchia FD, Drew MS (2000) A composite spectral model and its applications. In: The 8th color imaging conference, Scottsdale, pp 102–107
20. Mitchell M (1996) An introduction to genetic algorithms. MIT Press, Cambridge
21. Goldberg DE (1989) Genetic algorithms in search, optimization and machine learning. Addison Wesley, Reading
22. Angelopoulou E, Molana R, Daniilidis K (2001) Multispectral skin color modeling. In: IEEE conference on computer vision and pattern recognition. IEEE Computer Society Press, pp 635–642
23. Dupont D (2002) Study of the reconstruction of reflectance curves based on tristimulus values: comparison of methods of optimization. Color Res Appl 27(2):88–89
24. http://www.it.lut.fi/ip/research/color/database/database.html
25. http://www.cs.sfu.ca/~colour/data/colour_constancy_synthetic_test_data/index.html
26. ISO/TR 16066:2003, Standard object colour spectra database for colour reproduction evaluation (SOCS)